Enterotoxicity of a nonribosomal peptide causes antibiotic-associated colitis

Georg Schneditz[a], Jana Rentner[b], Sandro Roier[a], Jakob Pletz[b], Kathrin A. T. Herzog[c], Roland Bücker[d], Hanno Troeger[d], Stefan Schild[a], Hansjörg Weber[b], Rolf Breinbauer[b], Gregor Gorkiewicz[e], Christoph Högenauer[c,1], and Ellen L. Zechner[a,1]

[a]Institute of Molecular Biosciences, University of Graz, 8010 Graz, Austria; [b]Institute of Organic Chemistry, Graz University of Technology, 8010 Graz, Austria; [c]Division of Gastroenterology and Hepatology, Department of Internal Medicine and [e]Institute of Pathology, Medical University of Graz, 8036 Graz, Austria; and [d]Department of Gastroenterology, Infectiology and Rheumatology, Charité – Campus Benjamin Franklin, 10117 Berlin, Germany

Edited by Jon Clardy, Harvard Medical School, Boston, MA, and accepted by the Editorial Board July 28, 2014 (received for review February 21, 2014)

Antibiotic therapy disrupts the human intestinal microbiota. In some patients rapid overgrowth of the enteric bacterium *Klebsiella oxytoca* results in antibiotic-associated hemorrhagic colitis (AAHC). We isolated and identified a toxin produced by *K. oxytoca* as the pyrrolobenzodiazepine tilivalline and demonstrated its causative action in the pathogenesis of colitis in an animal model. Tilivalline induced apoptosis in cultured human cells in vitro and disrupted epithelial barrier function, consistent with the mucosal damage associated with colitis observed in human AAHC and the corresponding animal model. Our findings reveal the presence of pyrrolobenzodiazepines in the intestinal microbiota and provide a mechanism for colitis caused by a resident pathobiont. The data link pyrrolobenzodiazepines to human disease and identify tilivalline as a target for diagnosis and neutralizing strategies in prevention and treatment of colitis.

bacteria | enteric microbiota | cytotoxin

The human digestive tract houses several hundred microbial species (1). This complex community, known collectively as the intestinal microbiota, is important for human digestive physiology, immune function, and protection from pathogens (2). In healthy humans homeostasis between the microbiota and the host is maintained. Perturbed homeostasis, a state known as dysbiosis, is defined by shifts in bacterial abundances, their altered local distribution, and modified metabolic activities. Infections or nutritional or therapeutic stressors can induce dysbiosis and alter the integrity of the mucosal barrier. The pathogenesis of many disorders has been associated with dysbiotic changes in the intestinal microbiota, including metabolic diseases, cancer, allergies, and afflictions of the bowel, liver, and lung (3–6). The underlying mechanisms are poorly understood; however, recent work is beginning to show that microbial metabolites are important mediators of complex interactions between the enteric microbiota and the host. Thus, bacterial metabolites produced in a dysbiotic intestinal environment together with host factors may be important determinants in the pathogenesis of disease (7, 8).

Many drug therapies, and especially antibiotics, disrupt the human intestinal microbiota. Up to 30% of patients taking antibiotics experience diarrhea (9). With the exception of infection with toxin-producing *Clostridium difficile,* the underlying causes for the vast majority of diarrhea or colitis cases after antibiotic therapy are not known. A link to antibiotic-driven changes in microbial abundances and overgrowth of certain bacterial species is observed; however, the pathophysiological mechanisms remain to be determined (10). The expanding species are often not pathogens (11, 12) and in the majority of cases no single organism seems to explain either the presence or absence of disease.

In contrast to this general view, antibiotic-associated hemorrhagic colitis (AAHC) is a disease associated with antibiotic-driven enterobacterial overgrowth, which is dominated by a single organism, *Klebsiella oxytoca*. This bacterium is a resident of the gut in 2–10% of healthy individuals (13–15). In AAHC, a brief therapy with penicillins triggers dysbiosis with sudden onset of bloody diarrhea and abdominal cramps (14). *K. oxytoca* constitutively expresses resistance to amino- and carboxypenicillins (16). Antibiotic clearance of a niche in the colon facilitates overgrowth of *K. oxytoca* (10^7 cfu/g feces during acute phases of AAHC compared with 10^2 cfu/g feces in healthy subjects) (15). Our earlier work showed that the dysbiotic population shift dominated by *K. oxytoca* causes colitis (14), thereby identifying the resident organism as a pathobiont (17).

Here we aimed to characterize the pathogenicity of *K. oxytoca* in colitis. We identified the nonribosomal peptide tilivalline from *K. oxytoca* and demonstrate its causative action in an animal model of AAHC. Unlike most known enterotoxins, tilivalline is not a protein but a pyrrolobenzodiazepine metabolite not previously linked with the intestinal microbiota and human disease. Our findings define a mechanism whereby antibiotic-driven enterobacterial overgrowth and concomitant production of the small molecule enterotoxin ultimately leads to colitis.

Results

The *K. oxytoca* Cytotoxin Is Produced by Nonribosomal Peptide Synthetases. Secreted products of *K. oxytoca* strains isolated from AAHC patients have cytotoxic effects on human epithelial cells in vitro (13, 18–21). We asked whether the cytotoxic properties of *K. oxytoca* observed in vitro are important to development of the

Significance

The human gut microbiota is a complex community of microbes with enormous metabolic potential. Recognition of the significance of bacterial metabolites in mediating host interactions and the impact of perturbations of this ecosystem on human health has increased dramatically. Antibiotic therapy eliminates not only pathogens but also some of the commensal enteric microbiota, sometimes leading to inflammation and diarrhea. Understanding how microbial imbalance actually causes disease is challenging. This study reveals how a gut resident is able to cause colitis during penicillin therapy. We show that a pyrrolobenzodiazepine metabolite produced by *Klebsiella oxytoca* directly damages the intestinal epithelium and disrupts its protective barrier function. The enterotoxicity of tilivalline provides a mechanism for antibiotic-induced colitis.

Author contributions: G.S., H.T., S.S., R. Breinbauer, G.G., C.H., and E.L.Z. designed research; G.S., J.R., S.R., J.P., K.A.T.H., R. Bücker, and G.G. performed research; J.P. and H.W. contributed new reagents/analytic tools; G.S., R. Bücker, S.S., R. Breinbauer, G.G., C.H., and E.L.Z. analyzed data; and G.S. and E.L.Z. wrote the paper.

The authors declare no conflict of interest.

This article is a PNAS Direct Submission. J.C. is a guest editor invited by the Editorial Board.

Freely available online through the PNAS open access option.

Data deposition: The sequences reported in this paper have been deposited in the European Nucleotide Archive, EMBL (accession no. HG425356).

[1]To whom correspondence may be addressed. Email: christoph.hoegenauer@medunigraz.at or ellen.zechner@uni-graz.at.

This article contains supporting information online at www.pnas.org/lookup/suppl/doi:10.1073/pnas.1403274111/-/DCSupplemental.

disease. To identify *K. oxytoca* genes involved in cytotoxin production the clinical AAHC isolate AHC-6 (wild-type strain) was subjected to random Tn5 transposon mutagenesis. Mutants were analyzed for loss of toxicity toward cultured human epithelial Hep2 cells. Four of 1,500 mutants exhibited a toxin-negative phenotype (Fig. 1*A*) yet grew normally (Fig. S1*A*). The independent transposon insertion sites in toxin-deficient mutants were extracted and sequenced with adjacent chromosomal DNA. We identified the disrupted genes as a 2-keto-3-deoxy-D-arabino-heptulosonate-7-phosphate (DAHP) synthase gene we named *aroX* (Mut2), nonribosomal peptide synthetase (NRPS) genes *npsA* and *npsB* (Mut873, Mut89), and a 3-dehydroquinate-synthase gene *aroB* (Mut614) (Table S1). Assuming that *npsA* and *npsB* are part of an operon, we first created a nonpolar single-gene inactivation of *npsA* and then confirmed through complementation that both NpsA and NpsB gene products are required for toxin production (Fig. 1*B*).

NRPSs are multifunctional enzymes that link monomeric building blocks by a cascade of condensation reactions (22). The enzymes are organized as a modular set of enzymatic domains that are responsible for one discrete round of chain elongation and a variable set of modifications on each intermediate (Fig. 1*C*). The amino acid substrate is specifically selected and activated by the adenylation (A) domain followed by covalent attachment to the thiolation (T) domain. The condensation (C) domain joins the amino acids bound to T domains and the growing peptide chain translocates downstream. The first NRPS in an assembly line (initiation module) consists of only two domains: A and T. The last NRPS (termination module) includes a thioesterase (TE) or reductase (Re) domain to release the peptide from the NRPS enzyme complex, resulting in a C, A, T, TE/Re conformation (23). Application of the PKS/NRPS Analysis website tools (24) identified the bimodular NRPS domain architecture A, T, C, A, T, Re (Fig. 1*C*) whereby the T domain of the initiation module is atypically encoded by a separate gene, *thdA*, located between *npsA* and *npsB* (Fig. 1*D*). Conserved amino acid sequences of the NpsA and NpsB A domains (25) predict selective binding to pyrrole- and anthranilate-containing substrates, respectively (Fig. S2*A*). Inactivation of *aroB* (Mut614), but not *aroX* (Mut2), was lethal upon amino acid limitation, consistent with an essential function for AroB in the shikimate pathway (26, 27). The AroX isoenzyme seems to be produced in addition to the housekeeping DAHP synthases (AroFGH). The mutated paralog AroX (Mut2) was identified via sequence homology as a member of the type II DAHP synthase subclass that is insensitive to feedback regulation through aromatic amino acids (28). Apparent absence of feedback regulation for *aroX* agrees well with our observation that the cytotoxin is produced by *K. oxytoca* cultures grown in rich media containing aromatic amino acids.

The Toxin Gene Cluster Is Shared by Toxin-Positive *K. oxytoca*. The *K. oxytoca* AHC-6 genome was sequenced and annotated (EMBL accession no. HG425356). Three of the four mutated genes are clustered within a 7-kb region adjoining an asparagine tRNA gene (Fig. 1*D*). Comparison with other enterobacterial genomes revealed the location of the gene cluster to be a high-plasticity locus in the core genome typically harboring mobile DNA elements such as the polyketide synthase (*pks*) genotoxic island of

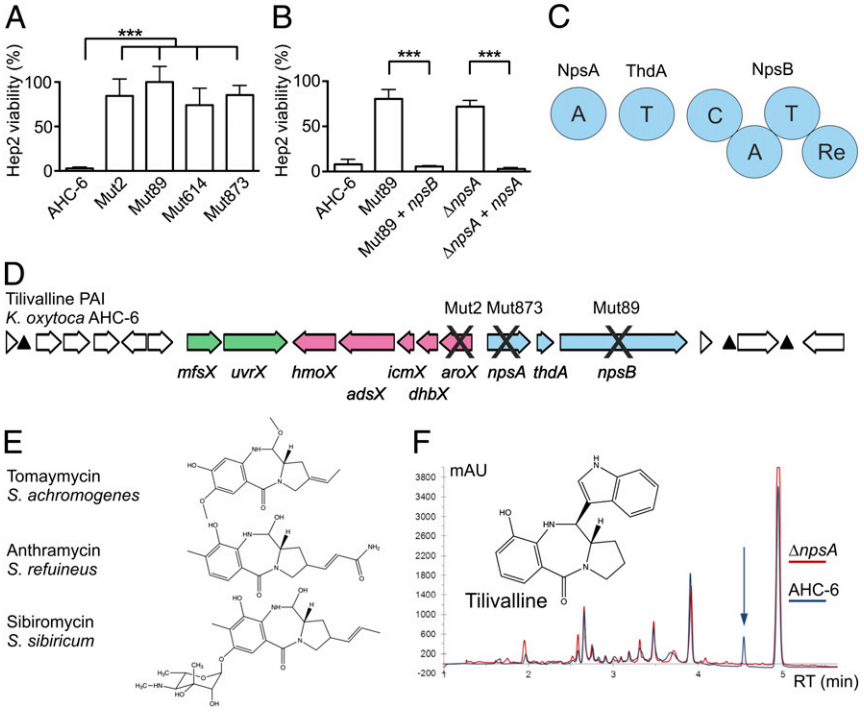

Fig. 1. Tilivalline, the *K. oxytoca* pyrrolobenzodiazepine cytotoxin, is synthesized by NRPSs related to those of Actinomycetes. (*A*) Conditioned media of *K. oxytoca* AHC-6 transposon mutants (Mut2, Mut89, Mut614, and Mut873) exhibit poor cytotoxicity toward Hep2 cells compared with AHC-6 in a MTT assay ($n = 3$). Statistical analysis was performed using the Mann–Whitney *U* test. ***$P \leq 0.001$. Values are means ± SD. (*B*) Toxicity of Mut89 (*npsB*::Tn5) and the *npsA* deletion mutant (Δ*npsA*) was complemented *in trans* with wild-type genes (+*npsB*) and (+*npsA*), respectively, compared with vector controls ($n = 6$). (*C*) Proposed bimodular assembly line of tilivalline comprising adenylation domains (A), thiolation domains (T), condensation domains (C), and thioester reductase domain (Re). (*D*) Tilivalline gene cluster highlighting putative functions: NRPS (blue), production of aromatic amino acid derivatives (red), transport (green), and unrelated genes (white). Genes inactivated in independent toxin-deficient transposon mutants are indicated (**X**). tRNA genes (▲) flank the PAI. (*E*) PBD products of homologous gene clusters are shown: tomaymycin (*Streptomyces achromogenes*), anthramycin (*Streptomyces refuineus*), and sibiromycin (*Streptosporangium sibiricum*). (*F*) Subtractive comparison of organic extracts of AHC-6 (blue) and Δ*npsA* (red) conditioned media identified a wild-type-specific compound at a retention time (RT) of 4.5 min. NMR spectroscopy established the structure of cytotoxin tilivalline.

Escherichia coli and determinants for the siderophore system yersiniabactin (29–32). This genetic context implies that the toxin biosynthesis genes are part of a larger pathogenicity island (PAI). The *aroB* gene is not found within this region, consistent with its role in general metabolism. The *nps* genes are conserved in several sequenced strains of *K. oxytoca* and are specific for this species (Table S2). The occurrence of the PAI among clinical isolates of *K. oxytoca* and other *Klebsiella* species was assessed by PCR amplification of *npsB* and the intergenic region between *npsA* and *aroX*. Both PAI targets were detected in 100% (46/46) of the toxin producers tested and 13% (7/52) of toxin-negative strains. PAI sequences were not detected in other *Klebsiella* spp. (0/12).

The *K. oxytoca* Cytotoxin Is Identified as Tilivalline, a Pyrrolobenzodiazepine Related to Those of Actinomycetes. Unexpectedly, we did not identify homologs to the *nps* genes in other known pathogens. Siderophore-producing NRPS clusters from Gram-negative bacteria seem to be unrelated. Instead, the majority of *K. oxytoca* PAI genes resemble pyrrolobenzodiazepine (PBD) biosynthesis clusters present in Gram-positive bacteria (Fig. 1*D* and Fig. S2*B*). The *K. oxytoca* PAI genes show >50% amino acid sequence similarity to PBD synthesis genes from soil bacteria belonging to Actinomycetales, *Streptomyces* and *Streptosporangium* (Fig. S2*B*), which produce low-molecular-weight effector molecules with potent cytostatic activities (Fig.1*E*) (33–35). A capacity for production of other metabolites or virulence factors is not apparent within the PAI genes (Table S1). To test whether the *K. oxytoca* toxin belongs to the PBD substance class we purified and determined its structure. We applied conventional extraction methods for PBDs (35, 36) to conditioned media of AHC-6 wild-type strain and the Δ*npsA* mutant. HPLC-MS analysis identified a 333-Da substance exclusively present in the extract of AHC-6 (Fig. 1*F*). No other unique species were apparent in the comparison. Isolation of the *K. oxytoca* cytotoxin was achieved via semipreparative HPLC. An exact molecular weight of 333.1493 Da was determined, suggesting a molecular formula of $C_{20}H_{19}N_3O_2$. The structure was established by NMR spectroscopy as a pentacyclic PBD (Fig. 1*F* and Fig. S3). Comparison with known structures revealed that this substance, tilivalline, was isolated from an uncharacterized *Klebsiella* strain previously (37). We next confirmed unambiguously that the PBD isolated from AHC-6 was structurally identical to tilivalline by producing fully synthetic tilivalline (compound **10**, *Supporting Information*) in a total synthesis following the procedure of Nagasaka and Koseki (38) and comparing their spectroscopical and physicochemical properties (Figs. S3 and S4). The toxicity of tilivalline toward mammalian cell lines in vitro was reported earlier (39), yet, remarkably, tilivalline has not been connected to *Klebsiella* pathogenicity. We next determined that pure tilivalline exhibits an IC_{50} of 10 μM for Hep2 cells. No antimicrobial effects of tilivalline were observed in agar diffusion tests using a panel of Gram-positive, Gram-negative, and fungal organisms (Table S3).

Tilivalline-Producing *K. oxytoca* Cause Colitis and Epithelial Apoptosis in Vivo. Key features of AAHC upon endoscopy are segmental mucosal hemorrhage and mucosal edema affecting mainly the ascending colon and cecum (14, 40). Histology typically resembles that of colitis induced by toxin-producing bacteria. We applied a rodent model of AAHC (Fig. S5) to test whether tilivalline production by *K. oxytoca* is critical for development of colitis in vivo. Animals with a conventional microbiota restricted for opportunistic pathogens were chosen, as opposed to germ-free animals, to simulate the antibiotic-induced dysbiosis experienced by colitis patients taking penicillins. Combined therapy of penicillin with a nonsteroidal anti-inflammatory drug (NSAID) increases risk for development of AAHC (14, 40), and thus we included indometacin in the medication control. Mice were treated intraperitoneally with the penicillin derivative amoxicillin/clavulanate and s.c. with the NSAID indometacin. The animals were infected with *K. oxytoca* AHC-6 carrying a kanamycin resistance marker (Fig. S1*B*), the mutant lacking *npsB* (Mut89), or the complementation strain Mut89 +*npsB*. The combined effects of amoxicillin/clavulanate and indometacin treatment led to *K. oxytoca* overgrowth in the colon of infected mice as described previously (14). Tilivalline production conferred no advantage in colonization comparing mice infected with AHC-6, Mut89, and Mut89 +*npsB* (Fig. 2*A*). AAHC-related pathologies in the right colon were significantly increased in animals infected with the wild-type strain compared with noninfected animals of the medication control group (Fig. 2 *B* and *C*). We also found a significant reduction in the pathology of animals infected with the tilivalline-deficient strain (Mut89) compared with the tilivalline-producing wild-type strain (AHC-6). The severely attenuated virulence of Mut89 was complemented by *npsB* expression *in trans* over the course of the experiment (Fig. S6*A*), resulting in a significant increase in colitis compared with the tilivalline-deficient strain (Mut89) (Fig. 2 *B* and *C*). AAHC-related pathologies of the complementation group resembled those infected with wild-type bacteria (Fig. 2 *B* and *C*).

Histology of human AAHC is consistent with a toxin-induced epithelial damage accompanied by pronounced epithelial apoptosis (Fig. S5) (14). In the disease model we similarly observed significantly increased epithelial apoptosis in the colon of the AHC-6 infection group compared with animals of the Mut89 infection and noninfected medication control groups (Fig. 3*A*). Apoptosis in animals infected with tilivalline-positive strains was additionally visualized by immunohistochemical detection of activated caspase-3. The majority of apoptotic cells were shed into the cecum lumen (Fig. 3*B*). Providing Mut89 with *npsB* on a complementation plasmid resulted in significantly increased epithelial apoptosis compared with Mut89 infection (Fig. 3*A*).

We sought to confirm production of tilivalline in infected animals. An attempt to detect the metabolite in organic extracts of the cecal contents using analytical mass spectroscopy was negative

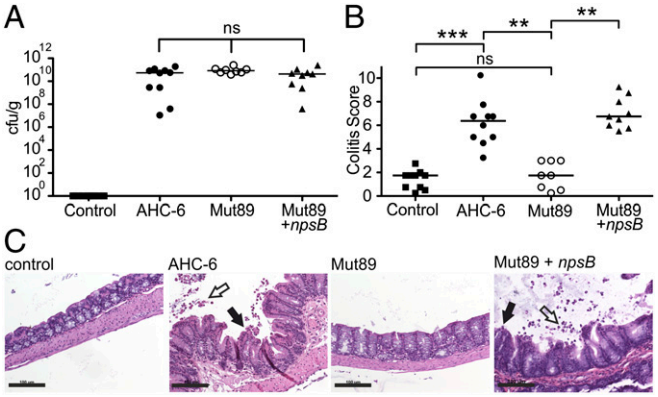

Fig. 2. Tilivalline-producing *K. oxytoca* cause colitis following penicillin treatment in mice. C57BL/6 mice were infected with *K. oxytoca* AHC-6 (n = 10), Δ*npsB* mutant Mut89 (n = 8), or Mut89 with *npsB* complementation +*npsB* (n = 9). Control animals received medication only (n = 10). Values are medians. (*A*) *K. oxytoca* in the cecum were enumerated by plating on selective differential agar (SCAI) (colony-forming units per gram of cecum). Statistical significance was determined using Kruskal–Wallis test and Dunn's post test. Ns (not significant), $P > 0.05$. (*B*) Colitis score (14) of murine cecal samples. Statistical significance was determined using Kruskal–Wallis test and Dunn's posttest. Ns (not significant), $P > 0.05$, $^{**}P \leq 0.01$, $^{***}P \leq 0.001$. (*C*) Hematoxylin/eosin-stained cecum sections of C57BL/6 mice from medication control and mice infected with AHC-6, Mut89, and Mut89 +*npsB*. Colitis is attenuated during infection with Mut89 and restored by Mut89 +*npsB*. Apoptotic cells are present in the lumen (open arrows) and as micropapillary protrusions of surface epithelia (filled arrows). (Scale bars: 100 μm.)

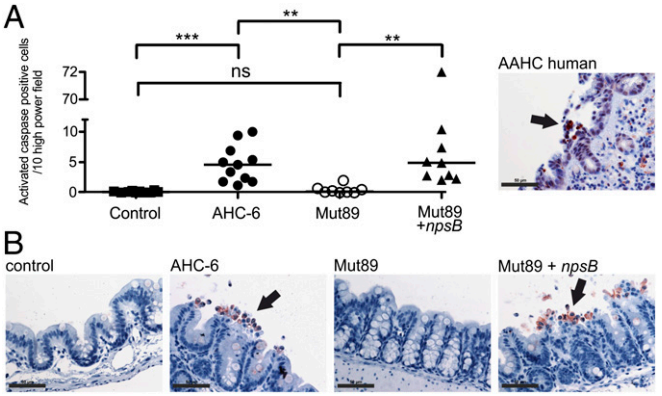

Fig. 3. Infection with tilivalline-producing *K. oxytoca* leads to epithelial apoptosis of murine epithelia. Cecum tissue originated from mice infected with *K. oxytoca* in the AAHC model. A human sample from an AAHC patient was included for comparison (upper right). (*A*) Apoptotic cells positively stained for activated capsase-3 were quantified. Statistical significance was determined using Kruskal–Wallis test and Dunn's posttest. Ns (not significant), $P > 0.05$, $^{**}P \leq 0.01$, $^{***}P \leq 0.005$. (*B*) Apoptotic cells (filled arrows) in cecum tissue sections of noninfected medication control mice and mice infected with AHC-6, Mut89, and Mut89 +*npsB* were visualized by immunohistochemical staining of activated caspase-3. (Scale bars: 50 μm.)

in all samples tested. The abundance of tilivalline in the host may be below the detection limit (~32 mM) we established for the metabolite added to feces (*Supporting Information*). Nonetheless, we reasoned that the sensitivity of human intestinal epithelial cells to tilivalline cytotoxicity in vitro should reveal a difference in the toxicity of cecal contents of animals infected with wild-type or mutant bacteria. Indeed cultured cells exposed to the cecal contents of animals infected with the tilivalline-producing wild-type (AHC-6) or complementation strain (Mut89 plus *npsB*) were significantly less viable compared with treatment with feces from animals carrying tilivalline-deficient strain Mut89 (Fig. S6*B*). Presence or absence of a single bacterial gene, *npsB*, is thus able to alter the cytotoxicity of the cecal samples of infected mice. We conclude that the specific virulence of *K. oxytoca* strains causing antibiotic colitis in the mouse model depends chiefly on tilivalline production.

Tilivalline Induces Caspase-3–Dependent Apoptosis in Vitro and Epithelial Barrier Dysfunction in Monolayers. Because toxin-producing wild-type and complemented infection strains, but not the toxin-deficient mutant, caused colitis in vivo, we next asked how intestinal epithelial cells are affected in vitro by tilivalline in the absence of *K. oxytoca*. The apoptotic cell death initiated by *K. oxytoca* was measured in Hep2 cells using activated caspase-3 staining and flow cytometry (Fig. 4 *A* and *B*). The percentage of apoptotic cells following exposure to AHC-6 conditioned medium (Fig. 4*A*) or purified tilivalline (Fig. 4*B*) surpassed that induced by the apoptosis activator staurosporine and was significantly higher compared with conditioned medium of the Δ*npsA* (tilivalline-deficient) strain.

Mechanisms underlying damage to the intestinal epithelium were evaluated with polarized T84 cell monolayers. Apical administration of tilivalline significantly lowered epithelial resistance (Fig. 4*C*) beginning 2 h after addition and reaching a minimum of 65% of the initial values after 20 h. No gross lesions were observed microscopically using nuclei and actin staining of treated monolayers. Preincubation of T84 monolayers with caspase inhibitor (Fig. 4*C*) eliminated the tilivalline-mediated effect. Tilivalline-induced apoptosis in this model was confirmed via TUNEL staining (Fig. 4*D*). We conclude that tilivalline disrupts the epithelial barrier via caspase-dependent apoptosis induction.

Discussion

The human microbiota produces numerous bioactive substances increasingly linked to the pathogenesis of intestinal and extraintestinal disorders. *K. oxytoca* is a resident of the enteric microbiota in 2–10% of healthy individuals (13–15). Alteration of the endogenous microbiota owing to penicillin treatment culminates in *K. oxytoca* overgrowth in the colon. Here we demonstrate that under these conditions strains that have acquired a genomic island specifying nonribosomal production of the cytotoxin tilivalline cause antibiotic-associated colitis. Cytotoxicity is thus a key attribute enabling this bacterium to act as a pathobiont. Our study highlights a direct link between biosynthesis of tilivalline in *K. oxytoca*, intestinal epithelial damage, and AAHC.

Nonribosomal peptides and polyketides represent two large families of structurally diverse microbial metabolites. Very few nonribosomal assembly lines in the Enterobacteriaceae have known functional roles. Among those are platforms involved in production of the iron-scavenging siderophores enterobactin and salmochelin, as well as the genotoxin colibactin, which is produced by a hybrid constellation of NRPS, polyketide synthases, and fatty acid synthases (41, 42). Surprisingly, the NRPS enzymes of *K. oxytoca* show little similarity to those of the Enterobacteriaceae but are closely related to synthases found in Actinomycetes. The structure of tilivalline is also highly similar to PBD antitumor antibiotics of *Streptomyces*, *Streptosporangium*, and *Micrococcus* species. Substances of this class share the PBD structural backbone, which is exclusively synthesized via NRPS (43). Most described PBDs are secondary metabolites of Actinomycetes, with

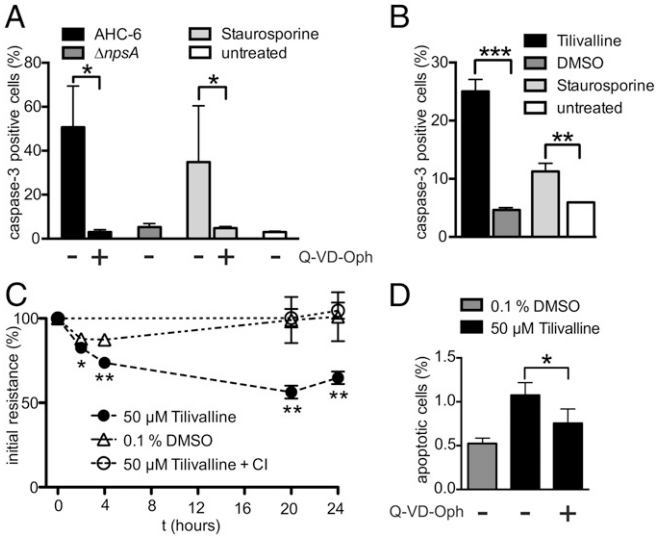

Fig. 4. Tilivalline induces caspase-3–dependent apoptosis in vitro and epithelial barrier dysfunction in monolayers. (*A*) Activated caspase-3–stained Hep2 cells after incubation for 24 h with conditioned medium of *K. oxytoca* AHC-6 or *K. oxytoca* Δ*npsA*, or 3 h with 1 μM apoptosis inducer (staurosporine). The additional absence or presence of 5 μM pan-caspase inhibitor Q-VD-Oph is indicated. (*B*) Caspase-3 activation after 12-h treatment with 50 μM tilivalline in 0.3% DMSO, DMSO only, or staurosporine. (*A* and *B*) ($n = 3$). Statistical significance was calculated using Mann–Whitney *U* test. Values are means ± SD; $^{*}P < 0.05$, $^{**}P < 0.01$, $^{***}P < 0.001$. (*C*) Tilivalline or solvent was added to the apical side of T84 cell monolayers. Transepithelial electrical resistance was measured via chopstick electrodes and values normalized to filter area. Changes were plotted as percentage of initial resistance. Tilivalline-induced loss of epithelial resistance was blocked by 5 μM Q-VD-Oph (CI) ($n = 3$). Values are means ± SD. Statistical significance was calculated using two-tailed Student *t* test. $^{*}P < 0.05$, $^{**}P < 0.01$. (*D*) Epithelial apoptosis in T84 monolayers was detected via TUNEL staining. Values were plotted as percent apoptotic cells per total cells ($n = 3$). Values are means ± SEM, two-tailed Student *t* test. $^{*}P < 0.05$.

the exception of pentacyclic PBDs that have been isolated from marine *Aspergilli* (44, 45). The origin of the genomic island carrying the tilivalline biosynthetic genes would thus seem to be phylogenetically distant. To our knowledge, tilivalline is the first PBD shown to be formed by the enteric microbiota and thus represents a new class of enterobacterial toxins.

We note with interest that the genetic context for insertion of the tilivalline gene cluster in the enterobacterial core genome is equivalent to the *asnW* tRNA locus occupied by the polyketide synthase (*pks*) genotoxic island in *E. coli* and some isolates of *Klebsiella pneumonia* (32, 42). The *pks* locus is highly conserved in the *E. coli* B2 phylogenetic group and an estimated 21% of humans carry colibactin-synthesizing *E. coli* in their intestinal microbiota (46). Mucosa-associated *pks*+ *E. coli* were found in a significantly high percentage of inflammatory bowel disease and colorectal cancer patients (46). The structure of colibactin is yet to be determined but its biological activity has been characterized (41, 47, 48). Colibactin damages DNA, inducing chromosome instability and mutations in host cells and may therefore contribute to colon cancer. This hypothesis is supported by a study showing *pks*+ *E. coli* promote tumorigenesis in a mouse model of colitis-associated colorectal cancer (46).

In an interesting functional parallel, the PBD monomers structurally related to tilivalline—anthramycin, sibiromycin, and tomaymycin—exert their cytotoxicity by covalent interaction with the minor groove of DNA (49). This bioactivity has driven development of PBDs as antitumor agents (50). The structure–activity relationships of PBDs are well understood (51). Presence of the indole substituent on the PBD scaffold suggests that tilivalline will not form a similar covalent DNA adduct. Nonetheless, tilivalline may interact with DNA. Here we show that part of tilivalline's pathophysiological effects on human epithelial cells is due to the induction of apoptosis. It will be important to address whether tilivalline production has antiproliferative or genotoxic effects on host cells. Its availability in the human intestine can be expected to vary from very low doses in healthy subjects to high levels during overgrowth and active phases of AAHC. Continuous low-level exposure of the intestinal epithelium to tilivalline may have consequences that range from tissue injury and inflammation of the colon to beneficial effects derived from antagonism of proliferative cells.

Understanding the functional relationship between the vast pool of secondary metabolites produced by the intestinal microbiota and host physiology is an important challenge; however, current knowledge is still very limited. *K. oxytoca* is exceptional in that it causes colitis in animals following antibiotic-induced disruption of the microbiota, conditions mirroring the etiology of AAHC in patients. Our observations support a model for the development of AAHC where exposure of the colonic epithelium to tilivalline during overgrowth of *K. oxytoca* creates apoptotic lesions and loss of the epithelial lining. Increased permeability of the breached epithelial barrier can lead to translocation of bacteria and bacterial antigens, increasing intestinal inflammation. Histopathology of tilivalline-induced colitis in the animal model resembles human AAHC. Medication alone (e.g., NSAID) can insult the colon epithelium, but only infection with tilivalline-producing *K. oxytoca* resulted in pronounced colitis in the disease model. In comparison, infection with tilivalline-deficient *K. oxytoca* resulted in minor intestinal inflammation without the epithelial apoptosis characteristic for AAHC. Concordant with the tilivalline-dependent histopathological changes, cecal contents recovered from animals infected with *K. oxytoca* were toxic to cultured epithelial cells in vitro in a manner dependent on gene *npsB*. Our findings thus establish a causal link for the bacterial cytotoxin tilivalline and AAHC in the dysbiotic intestine. Further study with this model will bring detailed understanding of colitis caused by *K. oxytoca* overgrowth and identify the interplay between the bacterial cytotoxic metabolite tilivalline and host physiology.

Methods

Standard methods and materials are described in *Supporting Information* and Tables S4–S6.

Isolation and Characterization of Tilivalline. Conditioned medium of *K. oxytoca* was extracted with *n*-butanol. After layer separation, the organic layer was dried over Na_2SO_4 and filtered and the solvent was evaporated at exactly 40 °C under reduced pressure. The crude powder was purified by semipreparative reversed phase HPLC (A: H_2O, B: MeOH, room temperature, 14 mL/min, 0–9 min: 40% B constant, 9–26 min: 40–50% B, 26–32 min: 50% B constant, λ_{max} = 221, 331 nm, t_R = 27 min) to yield a colorless solid, identified as (11***S***,11a***S***)-1,2,3,10,11,11a-hexahydro-9-hydroxy-11-(1***H***-indol-3-yl)-5***H***-pyrrolo[2,1-***c***][1,4] benzo-diazepin-5-one (tilivalline).

AAHC Mouse Model. Restricted flora C57BL/6 mice were housed in individually ventilated cages in the barrier facility at the Institute of Molecular Biosciences, University of Graz. Experimental animals were 8–9 wk old. Studies were performed in accordance with the Commission for Animal Experiments of the Austrian Ministry of Science (GZ 66.007/0006-II/3b/2011) and recommendations of the local ethics committee. Wild-type *K. oxytoca* AHC-6 was isolated from stool of an AAHC patient in the acute phase of colitis (14). Wild-type and mutant strains of AHC-6 carried an additional kanamycin selection marker *aphA*. Mice received amoxicillin/clavulanate (100 mg/kg per treatment) intraperitoneally twice daily at t = 0, 8, 24, 32, 48, 56, 72, and 80 h. Indometacin (2.5 mg/kg per treatment) was given s.c. once daily at t = 24, 48, and 72 h. Mice were infected intragastrically with 1×10^9 cfu *K. oxytoca* once daily at t = 0, 24, and 48 h. Animals were killed on day 5 and the whole intestinal tract was removed. Samples were taken separately from proximal and distal small intestine, cecum, and colon. Colonization by *K. oxytoca* was quantified via plating of homogenized cecum tissue including fecal content on SCAI agar and selective CASO agar. Histological analysis was performed via light microscopy of hematoxylin/eosin-stained cecum sections and scored for characteristics of AAHC (intestinal inflammation, mucosal hemorrhage and epithelial alterations including increased rate of apoptosis and mitosis, loss of goblet cells, and anisonucleosis) as described (14) and illustrated in Fig. S5. Additionally, epithelial apoptosis was assessed via immunohistochemical staining of activated caspase-3–positive cells.

Epithelial Resistance. T84 cells were seeded on polycarbonate filters with a pore size of 3 μm. Media was replaced every 48 h. Experiments were performed with cell monolayers showing a transepithelial electrical resistance (TER) above 1,000 $\Omega\cdot cm^2$. Medium was changed to serum-free conditions before start of the experiments. After treatment of T84 monolayers with tilivalline, TER was determined at different time points by an epithelial volt ohmmeter with chopstick electrodes (EVOM; World Precision Instruments) and values were normalized to filter area.

Statistics. Mann–Whitney *U* test was used for MTT assay and caspase-3 activation assay, two-tailed Student *t* test for transepithelial resistance, and Kruskal–Wallis followed by Dunn's post test for colonization data, histology scores and fecal toxicity assays. A *P* value of less than 0.05 was considered significant.

Genome Sequence. *K. oxytoca* AHC-6 gene sequences were deposited in the European Nucleotide Archive, EMBL (accession no. HG425356).

ACKNOWLEDGMENTS. We thank M. Joainig, S. Schauer, and P. Wallace for their contributions to this study. Research was funded by the Austrian Science Fund DK Molecular Enzymology (W901, to E.L.Z.), University of Graz, Medical University of Graz, NAWI-Graz, BioTech Med, and Oesterreichische Nationalbank (Anniversary Fund Project 14321, to C.H.).

1. Eckburg PB, et al. (2005) Diversity of the human intestinal microbial flora. *Science* 308(5728):1635–1638.
2. Sommer F, Bäckhed F (2013) The gut microbiota—masters of host development and physiology. *Nat Rev Microbiol* 11(4):227–238.
3. Karlsson FH, et al. (2013) Gut metagenome in European women with normal, impaired and diabetic glucose control. *Nature* 498(7452):99–103.
4. Yoshimoto S, et al. (2013) Obesity-induced gut microbial metabolite promotes liver cancer through senescence secretome. *Nature* 499(7456):97–101.

5. Olszak T, et al. (2012) Microbial exposure during early life has persistent effects on natural killer T cell function. *Science* 336(6080):489–493.
6. Schnabl B, Brenner DA (2014) Interactions between the intestinal microbiome and liver diseases. *Gastroenterology* 146(6):1513–1524.
7. Henao-Mejia J, et al. (2012) Inflammasome-mediated dysbiosis regulates progression of NAFLD and obesity. *Nature* 482(7384):179–185.
8. Russell WR, Hoyles L, Flint HJ, Dumas ME (2013) Colonic bacterial metabolites and human health. *Curr Opin Microbiol* 16(3):246–254.
9. Högenauer C, Hammer HF, Krejs GJ, Reisinger EC (1998) Mechanisms and management of antibiotic-associated diarrhea. *Clin Infect Dis* 27(4):702–710.
10. Stecher B, Maier L, Hardt WD (2013) 'Blooming' in the gut: How dysbiosis might contribute to pathogen evolution. *Nat Rev Microbiol* 11(4):277–284.
11. Ayres JS, Trinidad NJ, Vance RE (2012) Lethal inflammasome activation by a multidrug-resistant pathobiont upon antibiotic disruption of the microbiota. *Nat Med* 18(5):799–806.
12. Round JL, Mazmanian SK (2009) The gut microbiota shapes intestinal immune responses during health and disease. *Nat Rev Immunol* 9(5):313–323.
13. Beaugerie L, et al.; Infectious Colitis Study Group (2003) Klebsiella oxytoca as an agent of antibiotic-associated hemorrhagic colitis. *Clin Gastroenterol Hepatol* 1(5):370–376.
14. Högenauer C, et al. (2006) Klebsiella oxytoca as a causative organism of antibiotic-associated hemorrhagic colitis. *N Engl J Med* 355(23):2418–2426.
15. Zollner-Schwetz I, et al. (2008) Role of Klebsiella oxytoca in antibiotic-associated diarrhea. *Clin Infect Dis* 47(9):e74–e78.
16. Livermore DM (1995) beta-Lactamases in laboratory and clinical resistance. *Clin Microbiol Rev* 8(4):557–584.
17. Chow J, Tang H, Mazmanian SK (2011) Pathobionts of the gastrointestinal microbiota and inflammatory disease. *Curr Opin Immunol* 23(4):473–480.
18. Minami J, Okabe A, Shiode J, Hayashi H (1989) Production of a unique cytotoxin by Klebsiella oxytoca. *Microb Pathog* 7(3):203–211.
19. Joainig MM, et al. (2010) Cytotoxic effects of Klebsiella oxytoca strains isolated from patients with antibiotic-associated hemorrhagic colitis or other diseases caused by infections and from healthy subjects. *J Clin Microbiol* 48(3):817–824.
20. Higaki M, Chida T, Takano H, Nakaya R (1990) Cytotoxic component(s) of Klebsiella oxytoca on Hep-2 cells. *Microbiol Immunol* 34(2):147–151.
21. Herzog KA, et al. (2014) Genotypes of Klebsiella oxytoca isolates from patients with nosocomial pneumonia are distinct from those of isolates from patients with antibiotic-associated hemorrhagic colitis. *J Clin Microbiol* 52(5):1607–1616.
22. Marahiel MA (2009) Working outside the protein-synthesis rules: Insights into nonribosomal peptide synthesis. *J Pept Sci* 15(12):799–807.
23. Fischbach MA, Walsh CT (2006) Assembly-line enzymology for polyketide and nonribosomal Peptide antibiotics: Logic, machinery, and mechanisms. *Chem Rev* 106(8):3468–3496.
24. Bachmann BO, Ravel J (2009) Chapter 8. Methods for in silico prediction of microbial polyketide and nonribosomal peptide biosynthetic pathways from DNA sequence data. *Methods Enzymol* 458:181–217.
25. Stachelhaus T, Mootz HD, Marahiel MA (1999) The specificity-conferring code of adenylation domains in nonribosomal peptide synthetases. *Chem Biol* 6(8):493–505.
26. Srinivasan PR, Rothschild J, Sprinson DB (1963) The enzymic conversion of 3-deoxy-D-arabino-heptulosonic acid 7-phosphate to 5-dehydroquinate. *J Biol Chem* 238:3176–3182.
27. Herrmann KM, Weaver LM (1999) The shikimate pathway. *Annu Rev Plant Physiol Plant Mol Biol* 50:473–503.
28. Herrmann KM (1995) The shikimate pathway as an entry to aromatic secondary metabolism. *Plant Physiol* 107(1):7–12.
29. Buchrieser C, Brosch R, Bach S, Guiyoule A, Carniel E (1998) The high-pathogenicity island of Yersinia pseudotuberculosis can be inserted into any of the three chromosomal asn tRNA genes. *Mol Microbiol* 30(5):965–978.
30. Lin TL, Lee CZ, Hsieh PF, Tsai SF, Wang JT (2008) Characterization of integrative and conjugative element ICEKp1-associated genomic heterogeneity in a Klebsiella pneumoniae strain isolated from a primary liver abscess. *J Bacteriol* 190(2):515–526.
31. Schubert S, Dufke S, Sorsa J, Heesemann J (2004) A novel integrative and conjugative element (ICE) of Escherichia coli: The putative progenitor of the Yersinia high-pathogenicity island. *Mol Microbiol* 51(3):837–848.
32. Putze J, et al. (2009) Genetic structure and distribution of the colibactin genomic island among members of the family Enterobacteriaceae. *Infect Immun* 77(11):4696–4703.
33. Li W, Chou S, Khullar A, Gerratana B (2009) Cloning and characterization of the biosynthetic gene cluster for tomaymycin, an SJG-136 monomeric analog. *Appl Environ Microbiol* 75(9):2958–2963.
34. Li W, Khullar A, Chou S, Sacramo A, Gerratana B (2009) Biosynthesis of sibiromycin, a potent antitumor antibiotic. *Appl Environ Microbiol* 75(9):2869–2878.
35. Hu Y, et al. (2007) Benzodiazepine biosynthesis in Streptomyces refuineus. *Chem Biol* 14(6):691–701.
36. Hurley LH, Lasswell WL, Malhotra RK, Das NV (1979) Pyrrolo[1,4]benzodiazepine antibiotics. Biosynthesis of the antitumor antibiotic sibiromycin by Streptosporangium sibiricum. *Biochemistry* 18(19):4225–4229.
37. Mohr N, Budzikiewicz H (1982) Tilivalline, a new pyrrolo[2, 1-c][1,4] benzodiazepine metabolite from klebsiella. *Tetrahedron* 38(1):147–152.
38. Nagasaka T, Koseki Y (1998) Stereoselective synthesis of tilivalline(1). *J Org Chem* 63(20):6797–6801.
39. Shioiri T, et al. (1995) Structure-cytotoxicity relationship of tilivalline derivatives. *Anticancer Drug Des* 10(2):167–176.
40. Högenauer C, Hinterleitner T (2008) *Klebsiella oxytoca* as a cause of antibiotic-associated colitis. *Emerging Infections*, eds Scheld WMHS, Hughes JM (ASM, Washington, DC), pp 293–311.
41. Nougayrède JP, et al. (2006) Escherichia coli induces DNA double-strand breaks in eukaryotic cells. *Science* 313(5788):848–851.
42. Lai YC, et al. (2014) Genotoxic Klebsiella pneumoniae in Taiwan. *PloS ONE* 9(5):e96292.
43. Gerratana B (2012) Biosynthesis, synthesis, and biological activities of pyrrolobenzodiazepines. *Med Res Rev* 32(2):254–293.
44. Rahbaek L, Breinholt J (1999) Circumdatins D, E, and F: Further fungal benzodiazepine analogues from aspergillus ochraceus. *J Nat Prod* 62(6):904–905.
45. López-Gresa MP, et al. (2005) Circumdatin H, a new inhibitor of mitochondrial NADH oxidase, from *Aspergillus ochraceus*. *J Antibiot (Tokyo)* 58(6):416–419.
46. Arthur JC, et al. (2012) Intestinal inflammation targets cancer-inducing activity of the microbiota. *Science* 338(6103):120–123.
47. Cuevas-Ramos G, et al. (2010) *Escherichia coli* induces DNA damage in vivo and triggers genomic instability in mammalian cells. *Proc Natl Acad Sci USA* 107(25):11537–11542.
48. Secher T, Samba-Louaka A, Oswald E, Nougayrède JP (2013) Escherichia coli producing colibactin triggers premature and transmissible senescence in mammalian cells. *PloS ONE* 8(10):e77157.
49. Hurley LH, Gairola C, Zmijewski M (1977) Pyrrolo(1,4)benzodiazepine antitumor antibiotics. In vitro interaction of anthramycin, sibiromycin and tomaymycin with DNA using specifically radiolabelled molecules. *Biochim Biophys Acta* 475(3):521–535.
50. Hartley JA (2011) The development of pyrrolobenzodiazepines as antitumour agents. *Expert Opin Investig Drugs* 20(6):733–744.
51. Hurley LH (1977) Pyrrolo(1,4)benzodiazepine antitumor antibiotics. Comparative aspects of anthramycin, tomaymycin and sibiromycin. *J Antibiot (Tokyo)* 30(5):349–370.